Proceeding of the 7th International Symposium on Artificial Intelligence, Robotics and Automation in Space: i-SAIRAS 2003, NARA, Japan, May 19-23, 2003

Approach Planning and Guidance for Uncontrolled Rotating Satellite Capture Considering Collision Avoidance

Shuichi Matsumoto NASDA*/MIT** matsumoto.shuichi@nasda.go.jp
Stephen Jacobsen MIT** jacobsen@mit.edu
Steven Dubowsky MIT** dubowsky@mit.edu
Yoshiaki Ohkami NASDA* ohkami.yoshiaki@nasda.go.jp
* 2-1-1 Sengen, Tsukuba, Ibaraki, 305-8505, Japan
** 77 Massachusetts Ave., #3-469, Cambridge, MA, 02139, USA

Keywords Space Robotics, Satellite Capture, Path Planning, Approach, Guidance and Control

Abstract

The problem of planning safe kinematic approach trajectories for robotic capture of an uncontrolled rotating satellite is addressed, and two methods of trajectory planning are presented. The first method uses equations of orbital mechanics to plan a passive fly-by approach path for certain conditions of target satellite motion. The second method uses optimization techniques to plan an approach trajectory that is optimized with respect to a set of performance metrics. Results of these methods for representative scenarios are presented, and the relative merits of each method are discussed.

1. Introduction

The use of robotic technology for on-orbit satellite capture has been demonstrated and space robotics are likely to play an increasing role in satellite servicing missions in the future. The Shuttle Remote Manipulator System (SRMS), carried by the Space Shuttle and operated by an astronaut, has been used for satellite capture missions[1]. Engineering Test Satellite VII (ETS-VII) demonstrated cooperative satellite capture by a tele-operated manipulator[2] in 1999. While the technologies demonstrated by these missions can be used for certain satellite capture missions, their use is limited to the capture of satellites that are cooperative and attitude stabilized. For Example, the SRMS failed to capture the Spartan satellite that lost attitude control and was rotating at about 2 deg/s during the STS-87 mission in 1997. Thus, more advanced robot systems and planning and control algorithms are required for uncontrolled satellite capture[3,4].

An agile space robot supported by a mother space vehicle, such as the Hyper-OSV[5], is one advanced robotic solution that could be used. While a number of planning and control methods have been developed for space robots[6,7,8,9], new approach planning methods are required for uncontrolled satellite capture.

The Space Shuttle and ETS-VII have used a straight path approach[10,11] for the final approach to stable targets such as the International Space Station (ISS) and three-axis attitude controlled satellites. However, for general satellite capture missions, we cannot assume that the target satellite is in stable attitude nor that the docking or grasp point is fixed on a straight approach line. Thus we have developed two alternative approach methods for satellite capture.

This paper focuses on approach planning and guidance for uncontrolled rotating satellite capture considering issues such as collision avoidance between space robots and the target satellite, orbital mechanics, and realistic constraints such as controller capability, sensor error, actuator limitation and plume impingement. This work has been done as a part of a joint MIT and NASDA research project for advanced space robot planning and control methods, and this paper describes some of the results from the joint research.

2. Overview of Satellite Capture Mission

The sequence of tasks necessary for satellite capture[5] is shown in Fig.1 and can be roughly described as follows. At about 30-100m from a target satellite, space robots observe the target satellite motion and estimate its dynamic states such as quaternion and angular velocity vector (*Target motion estimation*). Using the estimated motion parameters, a space robot makes a capture plan considering satellite motion, lighting conditions, collision avoidance, error compensation ability and so on (*Task planning for capture*). The robot approaches the target on a safe path (*Safe approach*) and uses its manipulator to compensate for position and velocity errors during approach phase and capture the grasping point on the target satellite (*Capturing manipulation*). After the grasp, the space robot damps out the relative motion between the robot and the target satellite (*Relative motion control*).

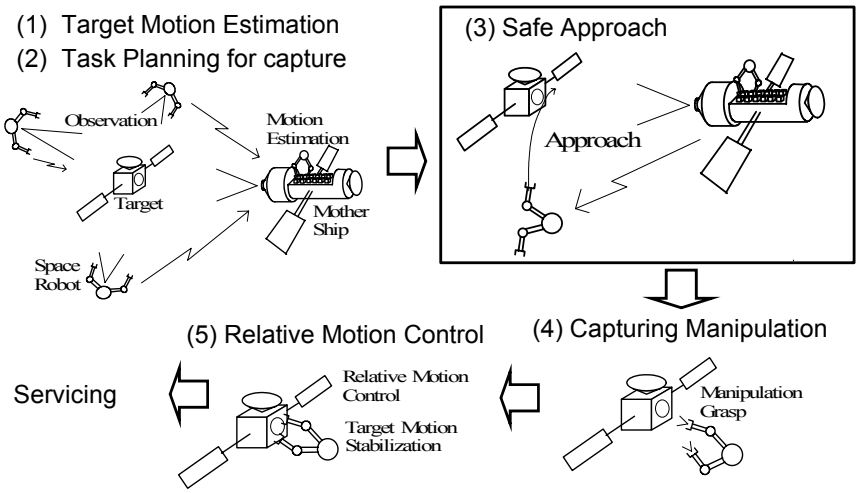

Fig. 1 Sequence of Satellite Capture

3. Fly-by Approach using Orbital Mechanics

3.1 Outline of Fly-by Approach

Figure 2 illustrates the sequence of phases during the fly-by approach. A space robot can start the transfer maneuver phase from an arbitrary position and execute the transfer maneuvers to match its position and velocity with the initial conditions for the fly-by approach at the appropriate time (*Transfer maneuver phase*). The CW guidance law can be used for the transfer maneuvers. During this phase, the robot's attitude and manipulator configuration should be prepared for capture manipulation. After injection for the fly-by approach trajectory, the space robot executes the trajectory adjusting maneuvers to compensate for position, velocity and timing errors due to the transfer maneuver and motion estimation (*Trajectory adjusting phase*). Reference trajectory guidance may be suitable for these maneuvers. While in close proximity to the satellite, the space robot should restrict thruster firing to avoid plum impingement on the satellite and panels. For this reason, in the fly-by approach, space robot approaches to the target on a passive trajectory resulting from orbital mechanics (*Fly-by approach phase*). To reduce interactive forces and torques during capture, the approaching velocity at the closest point of fly-by is matched with the velocity of grasping point on the target satellite at grasping time. If there are no system failure and the capturing conditions are satisfied, the space robot executes capturing manipulation, absorbs the relative position and timing error, and grasps a secure point on the target satellite. If a system failure or unexpectedly large error occurs, the space robot does not execute the capturing manipulation and escapes from the target satellite without any additional collision avoidance maneuver (*Fly-by escape phase*)

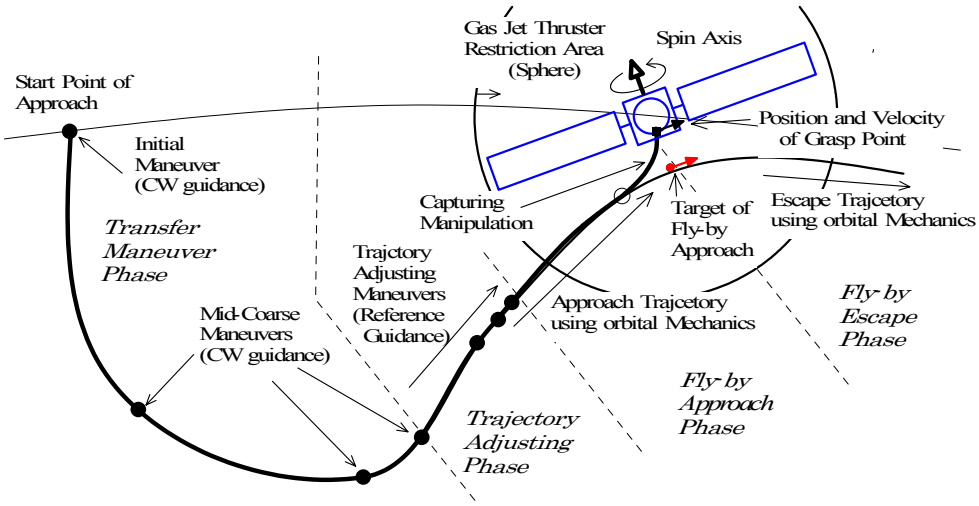

Fig. 2 Fly-by approach to target satellite

3.2 Relative Motion Due to Orbital Mechanics

The Hill's coordinate system[12,13] is used to express the relative motion of the space robot (chaser) with respect to the target satellite (target). The Hill's coordinate system is a rotating coordinate system with the orbital rate of the target. The origin is at the center of mass of the target. With its Z axis toword the center of the Earth and X axis tangential to the direction of travel of the target. Figure 3 shows the definition of the Hill's coordinate system using in this paper. Using this coordinate system, the relative motion dynamics between the chaser and target can be simplified as in Equation (1). If there are no external forces, the relative motion can be divided in-plane motion (x and z coordinates) and out-of-plane motion (y coordinates).

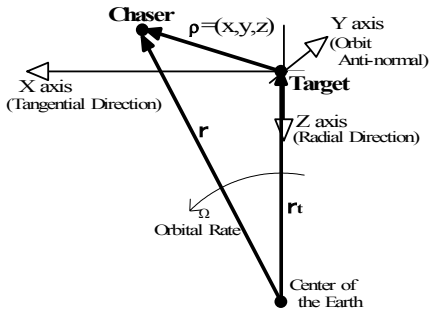

· Position of Chaser: $\boldsymbol{\rho}=\mathbf{r}-\mathbf{r}_t=[x, y, z]^T$
· Rotation of the Coordinate system:
$\boldsymbol{\Omega}=[0 \ -\Omega_t \ 0]^T$ Ω_t : Orbital rate of Target

Fig.3 Hill's Coordinate system

$$\ddot{x} = 2 \cdot \Omega_t \cdot \dot{z} + A_x \quad (1a)$$
$$\ddot{y} = -\Omega_t^{\,2} \cdot y + A_y \quad (1b)$$
$$\ddot{z} = -2 \cdot \Omega_t \cdot \dot{x} + 3 \cdot \Omega_t^{\,2} \cdot z + A_z \quad (1c)$$

where A_x, A_y, A_z *are external accelerations*

3.3 In-plane Relative Motion

In the case of no external accelerations, Equation (1) can be described in a vector form as Equation (2). Since the orbital rate, Ω_t, is much smaller than the relative velocity, $\dot{\boldsymbol{\rho}}$, the colioris force, the first term of the right-hand side of Equation (2), dominates the chaser's translational motion in the proximity zone.

$$\ddot{\boldsymbol{\rho}} = -2 \cdot \boldsymbol{\Omega} \times \dot{\boldsymbol{\rho}} + \Omega_t^{\,2} \cdot [0 \quad -1 \quad 3] \cdot \boldsymbol{\rho} \quad (2)$$

Since the orbital velocity vector, $\boldsymbol{\Omega}$, is on the −y-axis of Hill's coordinate system, the colioris force effects only in-plane relative motion and free-floating approach path is curved in the right-handed screw direction with respect to +y-axis. For the satellite capture problem, since the grasp point on the target satellite is rotating around the angular velocity vector of the target satellite, the relationship between the grasp point and approach path projected to the x-z plane is illustrated in Fig. 4. Even though we need to examine a safe approach to the target satellite in three dimensions, we can intuitively see that this effect of orbital mechanics could be useful for planning the safe approach if the appropriate conditions are chosen. For example, if we choose the grasp point at point G in Fig.4, which also determines the grasp time, the chaser can approach from and escape to an area away from the target satellite.

To see this in-plane relative motion behavior for the fly-by approach, an in-plane relative motion simulation was performed. In the simulation it was assumed that the target satellite was spinning along to the z-axis of Hill's coordinates. The target position and velocity of fly-by approach, X_t and V_t, are shown in Fig. 5. By choosing appropriate target condition, we can get a non-collision path in which the space robot approaches from a safe zone and also escapes to safe zone as shown in Fig.6. Figure 7 shows the relative position between the approach trajectory and region where a collision with the target satellite body or solar panels could occur, represented by cylinder in the figure. From Fig.7, we can confirm that the approach trajectory is a non-collision-path.

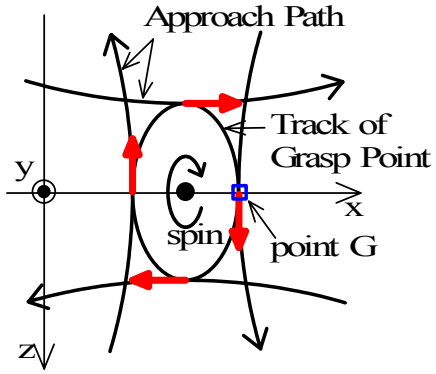

Fig.4 Grasp point velocity and approaching path

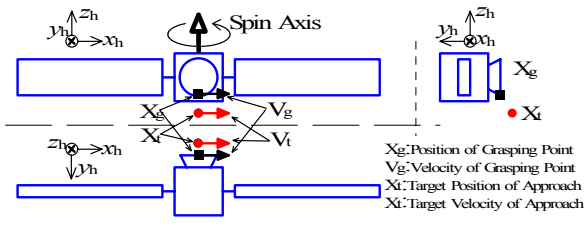

- Target Spin axis: +z axis of Hill's coordinates
- $X_T=[0 \ -1.5 \ -1.5]$, $V_T=[v_t \ 0 \ 0]$ (v_t = 0.05m/s, 0.1m/s, 0.2m/s, 0.35m/s, 0.5m/s, 1m/s, 2m/s)

Fig. 5 Target position and velocity (In-plane motion)

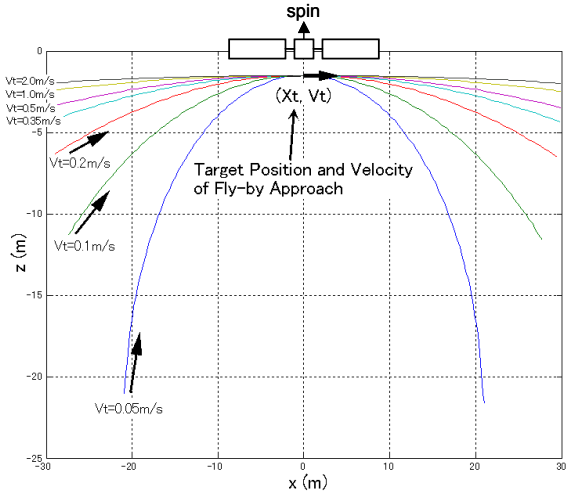

Fig.6 In-plane Motion Simulation result

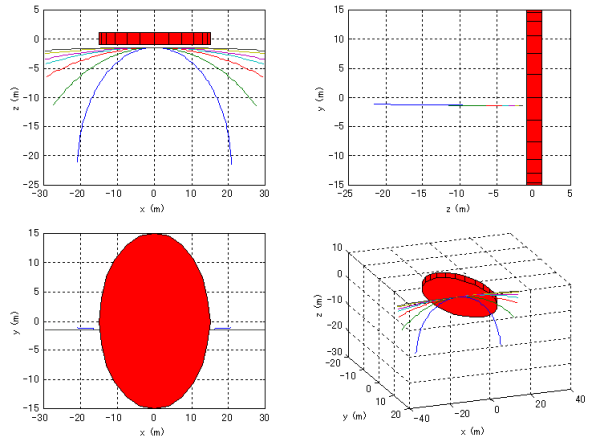

Fig.7 Relative position between approach trajectory and collision region (In-plane relative motion)

3.4 Out-of plane Relative Motion

From Equation (1b), we can see that motion in the y-direction is simple harmonic motion with a period of one orbital revolution, $T_{1rev} = \frac{2\pi}{\Omega_t}$. If there is no in-plane motion, which occurs in the case that the target velocity of proximity approach has only a y component and the target position has no z component, the relative motion is simple harmonic motion parallel to y-axis. This motion would be hazardous because if an approach vehicle loses its flight control system for some reason during the approach, the vehicle approaches closer to the target satellite once every orbital period due to orbital mechanics. Therefore, this purely out-of-plane relative motion should be avoided.

If the angular velocity vector of the target satellite is along the y-axis of Hill's coordinates, the case is a kind of singular point for the fly-by approach method. In this case, the approach path curves in a plane almost perpendicular to spinning axis and, if the target position is offset in the y direction, the space robot comes slightly closer to the target satellite before and after the target position because of orbital mechanics. To see this out-of-plane relative motion behavior for the fly-by approach, an out-of-plane relative motion simulation was performed with the following conditions:

- Target spin axis: +y-axis of Hill's coordinates
- X_t=[-1.5 -1.5 0]
- V_t=[0 0 v_t](v_t = 0.05m/s, 0.1m/s, 0.2m/s, 0.35m/s, 0.5m/s, 1m/s, 2m/s)

Figure 8 shows the out-of-plane simulation results. From Fig. 8, we can see that the approach path curves in the plane almost perpendicular to the y-axis, which is the spin axis. Even though the approach path is non-collision path, it provides no advantage in term of safety in this case. We can also see that the approach path and escape path are slightly closer to the collision region than the target position of the approach. Since the amount of this change is small, we can choose a non-collision path by considering an appropriate offset and solar panel length as shown in Fig.8. However, for the sake of safety, we should avoid this situation by choosing an appropriate grasping time and select the target position and velocity such that the space robot makes maximum use of in-plane convex approach motion.

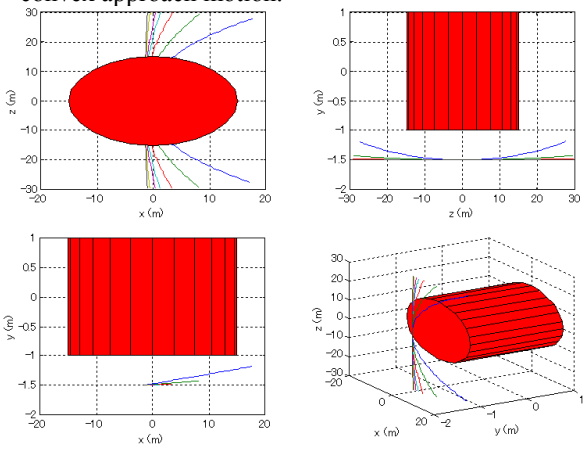

Fig.8 Relative position between approach trajectory and collision region (Out-of-plane relative motion)

3.5 Target Position and Velocity Determination

As discussed above, for fly-by approach we should avoid out-of-plane motion and use in-plane motion as much as possible in order to maximize the curvature of the convex approach trajectory. Since the grasp point on the target satellite is rotating around the satellite spin axis, we can choose a grasp time when the grasp point velocity has no y-component. For this condition, there are two solutions that satisfy this condition, and we should chose one such that the approach trajectory does not cross the target satellite collision region.

4. Approach Trajectory Planning Using Numerical Optimization Methods

4.1 Planning Methods[14]

In order to cope with more complicated constraints such as targets with complex shapes, large space objects, and multiple robot systems, a trajectory planning method based on optimization techniques has also been developed. Optimization based trajectory planning is accomplished through three basic steps. First, the approach trajectory is expressed in terms of parameters that describe its kinematic shape along its course. Second, a cost function is defined, which evaluates the quality of the approach trajectory based on performance metrics. Finally, an optimization routine determines the values of the path parameters that yield the lowest total cost and, therefore, the optimal approach trajectory.

The performance metrics used in the cost function include important factors during satellite approach, such as safety, fuel usage, and total time required. Physical system constraints, such as maximum thruster force, can also be represented in the cost function. Preliminary analysis indicates that reasonable approach times and fuel consumption can be achieved using realistic thrusters, but maximizing safety during approach remains a critical concern.

The safety of an approach trajectory is more difficult to quantify than conventional performance metrics, such as fuel usage or time. There are many possible measures of safety during approach, such as distance to the satellite and its panels or time within an area close to the satellite. Using each of these in the cost function will produce a different choice of optimal path.

Metrics used for the cost function in this study are:

1. Safety – measures relative velocity and distance in direction of satellite and panels and applies a penalty proportional to $v_{r\to s}^2/d_{r\to s}$ as shown in Fig. 9
2. Actuator limitations – limits acceleration along trajectory to less than maximum possible acceleration
3. Fuel – estimates fuel usage based on acceleration, mass of the robot, and specific impulse of fuel
4. Plume impingement – adds a cost proportional to acceleration away from the satellite and panels when the robot is within a certain distance
5. Time – proportional to the total approach time squared

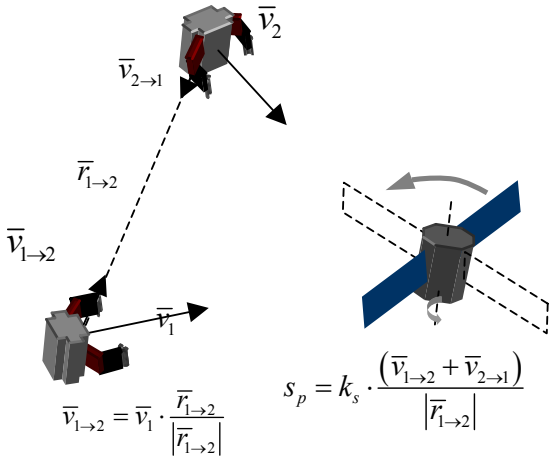

Fig. 9 Safety Metric Based on Relative Velocity and Distance

The approach trajectory of the robot is defined by

$$T = f(\mathbf{v}) \tag{3}$$

where f is the form of path representation, and $\mathbf{v}$ is the vector of path parameters. In its most general form, the parameterization specifies both the trajectory of the robot body and the robot configuration at each point in time. In this study, a subset of the general case is addressed; the translational position and velocity is accounted for by the path parameterization, but not the angular position or configuration of the robot.

In general, the cost function to be optimized consists of a path integral and additional functions of path parameters

$$P(\mathbf{v}) = \int_{t_0}^{t_f} f_1(v) + f_2(v) + \ldots dt + g_1(v) + \ldots \tag{4}$$

based on performance metrics f_i and g_i. The cost function should be a smooth function of the path parameters so that the minimum cost can be readily found by an optimization routine.

For this study, the cost function was discretized for numerical optimization as

$$P(\mathbf{v}) = \sum_{m} (k_a a_p + k_f f_p + k_s s_p + k_{pi} pi_p)\Delta t + k_t t_r^2 \tag{5}$$

where m is the total number of time steps on the trajectory and k_i are weighting coefficients for the performance metrics.

The path is parameterized using polynomic splines with sufficient degrees of freedom on each spline section to match boundary conditions. Cubic splines or parabolic splines with an additional spline section

fulfill the requirements of position and velocity boundary conditions for trajectory planning, and the latter are used in calculations for this case. Waypoints on each spline section combine with the initial and final boundary conditions to fully define the path.

For the case presented here, the robot is treated as a point mass on the path in order to simplify evaluation of the cost function at each point. In the more generalized case, robot configuration and end-state boundary conditions can be parameterized to allow variation in the final grasp velocity and configuration.

If the cost function used by the optimization routine contains local minima within the parameter space and the optimization routine does not rigorously search for the globally optimum solution, then supplying different initial parameter values to the routine may result in different paths being chosen as optimal. These different solutions may be equally desirable if they are caused by the existence of symmetry and yield the same value when evaluated by the cost function. Separate locally optimal solutions may, however, differ drastically from one another in their total cost, and care must be taken in the selection of initial parameter values when working with a cost function known to possess local minima. For this reason, a heuristically determined collision free path should be chosen as a starting point for an optimization routine.

By perturbing the set of parameters $\mathbf{v}$ and evaluating $P_i(\mathbf{v}_i)$, the algorithm moves $\mathbf{v}_i$ in the direction that produces the largest decrease in P and iteratively finds the parameter set $\mathbf{v}^*$ which minimizes P

$$\mathbf{v}^* = \min_{\mathbf{v}}(P(\mathbf{v})) \tag{6}$$

The optimal trajectory is then described by

$$T^* = T(\mathbf{v}^*) \tag{7}$$

In this study, a numerical approach to optimization is chosen for flexibility, and because the general cost function is not suitable for closed-form minimization. The Nelder-Mead [*] minimization algorithm is used because it does not require an explicit representation of the gradient of $P(\mathbf{v})$, and is robust to the complex form of the cost function.

When the trajectory has been optimized for a given set of n waypoints, n is incremented and a new $P(\mathbf{v}^*)$ is found. This process is repeated while the addition of waypoints significantly improves the total cost of the path. When $\Delta P_{n \to n+1}$ falls below a specified tolerance, the stopping criteria is met and the optimization process is complete. The trajectory defined by the current parameter set is chosen as the optimal approach trajectory.

4.2 Results

The representative target satellite used in the optimization study is the same as the satellite in used for orbital mechanics approach planning. The satellite is in a stable spin about its principal axis of inertial with an angular velocity of 5 deg/sec in the direction of the unit vector

$$\hat{e}_\omega = \left[\frac{1}{\sqrt{3}} \quad \frac{1}{\sqrt{3}} \quad \frac{1}{\sqrt{3}}\right]^T \quad \text{(Fig. 10).}$$

Optimization Results for Single Robot

The robot is initially located on the satellite's orbit 50 meters in the v-bar direction, with zero velocity relative to the satellite. At the end of the approach trajectory, the robot has synchronized its motion with the satellite at an offset distance from the target grasp point in preparation for grasp and stabilization.

The approach trajectory produced by optimization for this representative case is shown in Fig. 10 and a summary of important trajectory data is given in Table 1. The value of the safety metric is plotted vs. time for the approach trajectory in Fig. 11. The metric reaches a maximum when the robot is closest to the satellite and panels, immediately prior to grasp.

Table 1 Summary of Trajectory Data

Time	58.9 sec
approx. fuel consumption	1.05 kg
maximum acceleration	0.138 m/sec^2

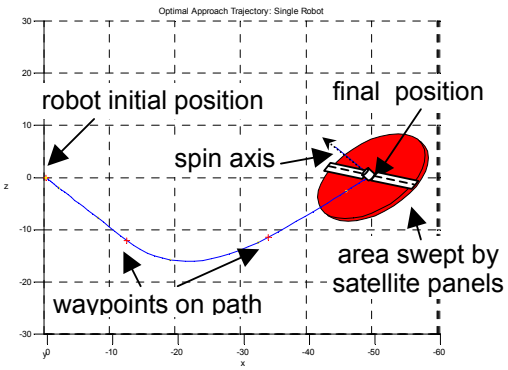

Fig. 10 Optimal Approach Trajectory for Single Robot, x-z plane

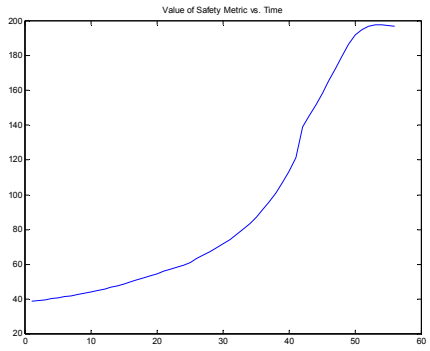

Fig,. 11 Value of Safety Metric vs. Time

Optimization Results for Multiple Robots

The optimization based trajectory planning method can be extended to the case involving multiple robots approaching a target simultaneously by evaluating the performance metrics for each body. By applying a safety metric to the relative motion between robots in addition to the relative motion of each robot with the target, the risk of collision between the robots can also be reduced.

In the representative case for multiple robots approaching simultaneously, the same target satellite is used and one robot starts at 50m in the + v-bar direction while the other is initially at 50m in the – v-bar direction. The results of optimization for these conditions is shown in Fig. 12, where the robots approach on opposite sides of the spin axis to avoid each other as well as the satellite panels.

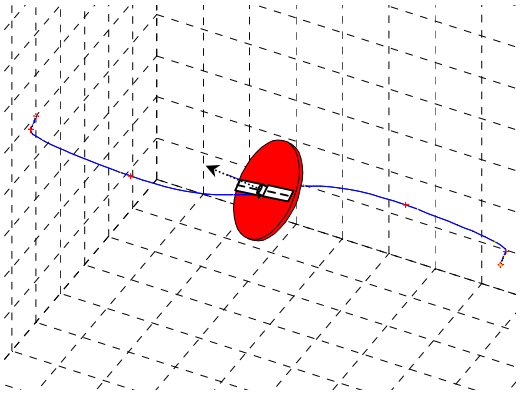

Fig. 12 Optimal Trajectories for Multiple Robots Approaching Simultaneously, x-z plane

5. Evaluation of Approach Planning Methods

The approach planning methods developed in this paper have relative advantages and disadvantages. Table 2 shows a comparison of two approach methods and Fig.13 shows the comparison of their applicable mission areas. Figure 14 shows the comparison of their simulation results under same conditions, showing similar trajectories for the conditions tested.

Table 2 Comparison of Two Approach Methods

	Fly-by Approach using orbital mechanics	Numerical Trajectory using safety metric
Applicable target motion	Angular Velocity: 0~ 3rpm	No restriction
Grasping point	Arbitrary direction	Arbitrary direction
Target Complexity	Satellite	Satellite, Large space structure, Multiple robots
Collision	Non-collision path	Probability of collision is very small
Thruster force, Fuel Consumption, Plume impingement	Smaller	Larger than Fly-by approach
Real-time guidance	Possible with existing space-born computer	Higher performance computer is required

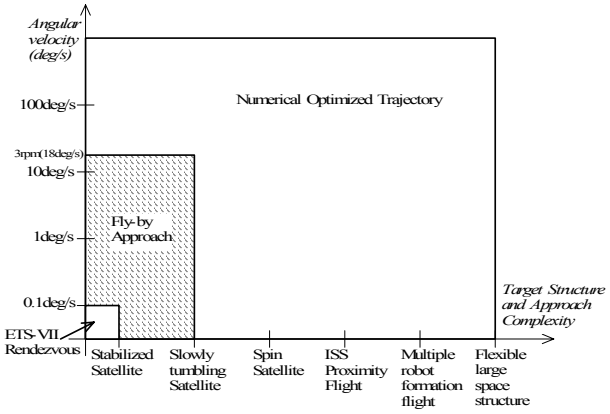

Fig.13 Comparison of Applicable Mission Area

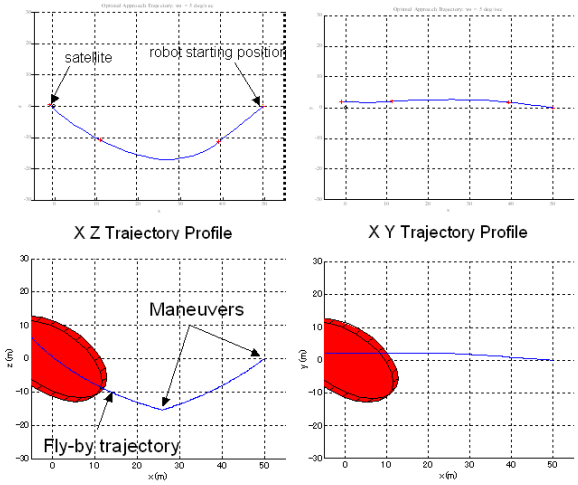

Fig.14 Comparison of Simulation results

6. Conclusion

This paper described two new approach methods; the "Fly-by approach using orbital mechanics" and the "Approach trajectory planning using numerical optimization methods", and discussed their advantages and limitations. Although more detail studies such as studies on error sensitivity and robustness to sensor and actuator limitation are necessary, basic approach planning and guidance method for uncontrolled rotating satellite capture have been developed.

References

1 Zimpfer, D., and Spehar, P., "STS-71 Shuttle/Mir GNC Mission Overview", Advances in the Astronautical Sciences, Vol.93, American Astronautical Society, San Diego, CA, 1996, pp.441-460; also AAS paper 96-129

2 Oda, M., "Experiences and lessons learned from the ETS-VII robot satellite", Proc. of the 2000 IEEE International Conference on Robotics and Automation (ICRA 2000), San Francisco, CA, April 2000

3 King, D., "Space Servicing: Past, Present and Future", Proc. of the 6th International Symposium on Artificial Intelligence and Robotics & Automation in Space (i-SAIRAS 2001), Montreal, Canada, 2001

4 Yoshida, K., "Space Robot Dynamics and Control: To Orbit, From Orbit, and Future", Robotics Research, The Ninth International Symposium, Eds, Hollerbach, J.M, and Koditschek, D.E, pp.449-456, Springer, 2000

5 Matsumoto, S., et. al., "Satellite Capturing Strategy Using Agile Orbital Servicing Vehicle, Hyper-OSV", Proc. of IEEE ICRA, 2002

6 Dubowsky, S., and Papadopoulos, E., "The Kinematics and Control of Multi-Manipulator Free-flying and Free-floating Space Robotics System", IEEE Transactions on Robotics and Automation, vol. 9, no. 5, 1993, pp. 1-13

7 Xu, Y. and Kanade, T., "Space Robotics: Dynamics and Control", Kluwer Academic Publishers, ISBN 0-7923-9265-5, 1992

8 Ullman, M. A., "Experiments in Autonomous Navigation and Control of Multi-Manipulator Free-Flying Space Robots" PhD thesis, Stanford University, Stanford, CA, 1993

9 Kawatmoto, S., Matsumoto, K., and Wakabayashi, S., "Ground Experiment of Mechanical Impulse Method for Uncontrollable Satellite Capturing", Proc. of the 6th International Symposium on Artificial Intelligence and Robotics & Automation in Space (i-SAIRAS 2001), Montreal, Canada, 2001

10 Kawano, I., et al., "First Results of Autonomous Rendezvous Docking Technology Experiments on NASDA's ETS-VII Satellite", IAF-98-A.3.09, 49th International Astronautical Congress, 1998

11 Pearson, D. J., "The Glideslope Approach", Advances in the Astronautical Sciences, Vol.69, American Astronautical Society, San Diego, CA, 1989, pp.109-123; also AAS paper 89-162

12 Clohessy, W., H., and Wiltshire, R., S., "Terminal Guidance System for Satellite Rendezvous", Journal of the Aerospace Sciences, Vol.15, September, 1960, pp.653-658

13 Sidi, M., J., "Spacecraft dynamics and control: a practical engineering approach," Cambridge University Press, 1997

14 Jacobsen, S., et. al., "Planning of Safe Kinematics Trajectories for Free-Flying Robots Approaching an Uncontrolled Spinning Satellite", Proc. of ASME DETC, Montreal, Canada, 2002

15 Sakawa, Y., "Trajectory planning of a free-flying robot by using the optimal control. Optimal Control Applications and Methods, 20, 235-248, 1999

16 Kindel, R., Hsu, D., Latombe, J., and Rock, S., "Kinodynamic motion planning amidst moving obstacles" IEEE International Conference on Robotics and Automation, 2000

17 Nelder, J. A. and Mead, R., "A Simplex Method for Function Minimization." Comput. J. 7, 308-313, 1965